ISSN 1062-8738, Bulletin of the Russian Academy of Sciences: Physics, 2021, Vol. 85, No. 6, pp. 647–652. © Allerton Press, Inc., 2021.
Russian Text © The Author(s), 2021, published in Izvestiya Rossiiskoi Akademii Nauk, Seriya Fizicheskaya, 2021, Vol. 85, No. 6, pp. 842–848.

Imaging in a Liquid through a Solid-State Acoustic Lens with Aberration Correction

S. A. Petrosyan[a, *], D. A. Nikolaev[a], S. A. Tsysar[a], V. D. Svet[b], A. I. Tsekhanovich[a], A. D. Krendeleva[a], and O. A. Sapozhnikov[a]

[a] *Faculty of Physics, Moscow State University, Moscow, 119991 Russia*

[b] *Andreyev Acoustics Institute, Moscow, 117036 Russia*

**e-mail: sa.petrosjan@physics.msu.ru*

Received December 9, 2020; revised January 25, 2021; accepted February 26, 2021

Abstract—A method of acoustic imaging in a liquid through a solid-state lens by using phase data processing with aberration correction is proposed. Results are presented from the theoretical modeling and the experimental study of investigating objects located in water.

DOI: 10.3103/S1062873821060198

INTRODUCITON

Problems of sonovision require the ultrasonic (US) imaging of objects located at a distance from a receiving/transmitting system. One-dimensional and two-dimensional receiving/transmitting phased antenna arrays are now used in many applications. When a studied domain is at a distance comparable to the array's diameter, high lateral resolution is achieved due to the angular width of the aperture. However, there are applications for which a receiving/transmitting system cannot be moved closer to the domain of visualization for one reason or another. One such example is US imaging in a corrosive liquid, when the array must be distant from the studied object and even placed into another medium. Conventional US technologies then give low-quality images because both the sounding and detection of scattered waves occur within a relatively narrow angular range. A possible solution in these situations is to use an acoustic lens system located in the vicinity of a visualized object. The range of sounding angles can be broadened considerably and the receiving/transmitting system can be located at a considerable distance from the lens without loss of the spatial resolution. The use of acoustic lenses and mirrors also allows us to control the direction of a probe pulse's propagation and scale the image, which lets us increase the size of the receiving elements without loss of image quality [1]. If the medium beyond the plane surface of the lens is optically transparent, remote optical techniques can be used to detect vibrations and find the amplitude distribution of the normal component of the vibration velocity directly at the plane lens surface using a laser Doppler vibrometer [2].

In this work, we propose a way of calculating the propagation of an acoustic field to construct a US image using pulse sounding through a thick lens while allowing for diffraction and refraction. We use two ways of analyzing the ultrasonic field based on Rayleigh integrals [3, 4] and an angular spectrum [5].

We developed an experimental setup to validate the proposed technique for constructing US images. A piezoelectric radiator placed in a liquid on whose surface a pattern of an absorbing material was mapped served as our object of visualization. A thick solid lens was positioned opposite this radiator. On the opposite side, ultrasonic signals were detected using a synthetic two-dimensional array of receivers. Synthesis was performed via raster scanning of a single hydrophone along the plane surface section. The two-dimensional distribution of the ultrasonic field detected by this array was used as input data for the developed theoretical algorithms of imaging.

THEORY AND MODELING

When irradiating an object with a probe acoustic pulse, the nonstationary acoustic signal scattered by inhomogeneties is detected by receivers that form a two-dimensional array. Imaging requires us to solve an inverse problem that can be reduced to the direct problem of propagation of acoustic waves from the receiving array to the object when the phase of the acoustic field received by the array is reversed. (For pulse signals, the time is reversed.) With an acoustic lens located between the object and receiving array, the object can be imaged using a thin-lens approximation [6]. With thick lenses that have a highly curved

surface, this approach results in aberration caused by the difference between the real and thin lenses.

The back propagation of a wave from the array through the lens to the domain of the object's location must be described more accurately to obtain a better (aberration-free) solution to the problem of imaging. Below, we propose using either Rayleigh integrals [3, 4] or an angular (spatial) spectrum [5] to recalculate the field in three domains. At the first step (I), we perform calculations from the measuring surface to the plane surface of the lens in water; at the second (II), we calculate the propagation of the field within the lens material from the plane to concave surface; and at the third (III), we recalculate the field from the concave lens surface in water to the plane of the object's location.

Extending the representation of the real wave function to the complex plane, we take the temporal part of the wave function describing a harmonic oscillation with frequency ω in the form $e^{-i\omega t}$.

Rayleigh Integrals

Let us consider a source of harmonic oscillations with frequency ω lying on the plane S_1. For a known pattern of oscillations with the distribution of the normal component of vibration velocity u or acoustic pressure P along plane S_1, the acoustic field at any point of a half-space with radius–vector $\vec{r}_2$ is described by Rayleigh integrals as

$$P\left(\vec{r}_2\right) = \frac{-i\rho\omega}{2\pi}\iint\limits_{S_1} u\left(\vec{r}_1\right)\frac{e^{ikR}}{R}dS_1, \quad (1)$$

$$P\left(\vec{r}_2\right) = \frac{1}{2\pi}\iint\limits_{S_1} P\left(\vec{r}_1\right)\frac{\partial}{\partial\vec{n}_1}\left(\frac{e^{ikR}}{R}\right)dS_1, \quad (2)$$

where $k = \frac{\omega}{c}$ is the wavenumber; ρ is the equilibrium density of the medium, P is the distribution of the acoustic pressure amplitude; $\vec{r}_1$ denotes the coordinates of points on surface S_1; $R = \left|\vec{r}_2 - \vec{r}_1\right|$ is the distance between point of observation $\vec{r}_2$ and surface element dS_1 with radius vector $\vec{r}_1$; and $\vec{n}_1$ is the unit normal of surface element dS_1, directed toward the observation point. Calculating the partial normal derivative over $\vec{n}_1$ and introducing an additional vector, we rewrite formula (2) as

$$P\left(\vec{r}_2\right) = \frac{1}{2\pi}\iint\limits_{S_1} P\left(\vec{r}_1\right)\left(\overrightarrow{m_{12}}\cdot\vec{n}_1\right)\left(\frac{ik}{R} + \frac{1}{R^2}\right)e^{ikR}dS_1, \quad (3)$$

where $\overrightarrow{m_{12}} = \left(\vec{r}_2 - \vec{r}_1\right)/R$ is the unit vector directed from surface element dS_1 with radius vector $\vec{r}_1$ toward point of observation $\vec{r}_2$ [7, 8]. However, if we reverse radiating surface S_1 and surface S_2, on which the acoustic pressure with radius-vector $\vec{r}_2$ must be reconstructed (i.e., the back propagation of a wave is considered), Eq. (3) will be equivalent if we substitute $i\omega$ for $-i\omega$ and $\vec{r}_1, \vec{r}_2, S_1, S_2$ for $\vec{r}_2, \vec{r}_1, S_2, S_1$, respectively.

Since in this problem we consider surfaces with a radius of curvature much larger than the characteristic wavelength of the probe pulse, the inaccuracy of the Rayleigh integral will be negligible and the solution will be fairly accurate with allowance for the diffraction limit [9].

Angular Spectrum

Angular (spatial) spectrum is widely used to solve scattering problems because of the convenience of plane-to plane calculations of the field. We use a plane-wave expansion of a field set on a surface and apply a two-dimensional spatial Fourier transform that allows us to analyze changes in the angular spectrum of radiation as it propagates in space [10, 11]. When using this technique, it is convenient to plot the US pattern in a plane removed at an arbitrary distance from the initial plane, the pressure distribution over which is experimentally measured using acoustic receivers. As was noted above, the presence of a lens between these planes requires us to calculate the field at the boundaries of domains, one of which is not flat (concave lens surface). It is therefore convenient to write the formulas for calculating the field not from plane-to-plane, but in a more general form for an arbitrary set of spatial points.

In contrast to Rayleigh integrals (1) and (2), which (as was noted above) express the field as superposition of radiation of the point sources located on surface S_1 at points $\vec{r}_1 = (x_1, y_1, z_1)$, the angular spectrum approach uses a plane-wave expansion. For the transition to this expansion, multiplier $\frac{e^{ikR}}{R}$ under the integral can also be generally expressed as an expansion over the angular spectrum in half-space $z_2 \geq z_1$ [12]:

$$\frac{e^{ik\left|\vec{r}_2 - \vec{r}_1\right|}}{\left|\vec{r}_2 - \vec{r}_1\right|} = \frac{i}{2\pi}\iint\limits_{-\infty}^{\infty}\frac{\exp\left[i\left(k_x(x_2 - x_1) + k_y(y_2 - y_1) + (z_2 - z_1)\sqrt{k^2 - k_x^2 - k_y^2}\right)\right]}{\sqrt{k^2 - k_x^2 - k_y^2}}dk_x dk_y. \quad (4)$$

After substituting (4) into formula (1), we obtain the expression for the amplitude of acoustic pressure:

$$P\left(\vec{r}_2\right) = \frac{1}{4\pi^2}\iint_{-\infty}^{\infty} S\left(k_x, k_y\right) e^{i\left(k_x x_2 + k_y y_2 + z_2\sqrt{k^2 - k_x^2 - k_y^2}\right)} dk_x dk_y, \quad (5)$$

where the angular spectrum is

$$S\left(k_x, k_y\right) = \frac{\rho c}{\sqrt{1 - \dfrac{k_x^2 + k_y^2}{k^2}}} \iint_{S_1} u\left(\vec{r}_1\right) \times e^{i\left(k_x x_1 + k_y y_1 + z_1\sqrt{k^2 - k_x^2 - k_y^2}\right)} dS_1. \quad (6)$$

To calculate the Rayleigh integral (2), the angular spectrum method is similarly used to expand multiplier $\dfrac{\partial}{\partial \vec{n}_1}\left(\dfrac{e^{ikR}}{R}\right) = \dfrac{\left(\left(\vec{r}_2 - \vec{r}_1\right)\cdot \nabla F\left(\vec{r}_1\right)\right)}{R\cdot\left|\nabla F\left(\vec{r}_1\right)\right|}\left(\dfrac{-ik}{R} + \dfrac{1}{R^2}\right)e^{ikR}$ over the angular spectrum in the half-space $z_2 \geq z_1$, where equation $F\left(\vec{r}_1\right) = 0$ is that of surface S_1. Note that the existence of evanescent (nonhomogeneous) waves is considered when $k_x^2 + k_y^2 > k^2$. These waves have a purely imaginary wavenumber and decay exponentially in the direction of positive z, but they can also be used along with a highly sensitive receiving facility [13]. These waves were not considered in this work.

Calculating the Field in the Thin-Lens Approximation

In this work, it was more convenient to use an angular spectrum to construct an image in the thin-lens approximation because it allowed us to perform fast plane-to-plane calculations of the field, since the physical curvature of the concave surface of the lens was ignored. The field from the receiving array surface to the thin lens surface must therefore be calculated (I); the effect of the focusing of the lens must be considered (II); and the field from the same lens plane to that of the location of the studied object must be calculated (III). Steps (I) and (III) are calculated using the angular spectrum.

The lens is considered at second step (II). Using the thin-lens approximation without aberrations, we first calculate the focal length for the plane-concave lens [6]:

$$F = \frac{R}{1 - \dfrac{c_1}{c_2}}, \quad (7)$$

where c_1 and c_2 are the speeds of ultrasound in the surrounding medium and the lens material, respectively; R is the radius of curvature of the concave surface of the lens. We next determined the coefficient of transmission for the thin lens, $T(x, y)$, while ignoring reflection and losses in the paraxial approximation ($x^2, y^2 \ll R^2$) [6], which represents the phase factor

$$T\left(x, y\right) = \frac{P_2\left(x, y, z_L\right)}{P_1\left(x, y, z_L\right)} = \exp\left(-i\frac{k\left(x^2 + y^2\right)}{2F}\right). \quad (8)$$

Here, P_1 and P_2 are the complex amplitude distributions of the acoustic pressure in the lens plane at the input and output (with respect to the receiving plane), respectively; x and y are the orthogonal coordinates in the lens plane; z is the coordinate in the direction normal to the lens plane; and $z = z_L$ is the lens plane.

Constructing a Model Image

For an initial check of imaging quality, we developed a numerical model in the form of a set of harmonic in-phase point sources at a frequency of 1.5 MHz in the focal plane of the lens. The distances between sources were 1, 2, 3, and 4 mm (Fig. 1a). Using this model, we calculated the field at the surface beyond the lens, which modeled the surface of the receiving array in the experiment. The obtained data were then used as the boundary conditions to solve the inverse problem of wave propagation and construct a US image of the given set of the point sources using the procedures described above (Rayleigh integral, angular spectrum, and thin-lens approximation).

The set of the input data for solving the inverse problem was calculated using ray tracing from each point source. The ray path of propagating through the lens was calculated by allowing for refraction according to Snell's law, and reflection according to the Fresnel formulas for the coefficient of transmission of a longitudinal wave. Shear waves were ignored, since only a longitudinal wave corresponded to the first transmitted signal (pulse), which was subsequently used to construct an image in the experiment. Form each point of the scatterer, approximately 10^5–10^6 rays fell on the lens surface. These were then analyzed on a receiving plane located at a distance of 29.4 mm from the plane lens surface. According to ray acoustics, the intensity of rays falling into a square grid cell with a side of $\lambda/2$, where λ is the wavelength in a liquid, was re-calculated to the amplitude of the transmitted wave, and the delay along the ray was recalculated to the wave phase. These calculations were performed for all point scatterers. The obtained distributions of the complex amplitude of each point source were then summed, yielding the required two-dimensional field distribution for the set of point sources.

The second stage of modeling consisted of constructing images of the point sources using the procedures described above. The geometry of the model coincided with that of the experiment (Fig. 2a). At first step (I), the distribution of the acoustic pressure at the plane lens surface was reconstructed with a lateral step of 0.5 mm using Rayleigh integral (2) and

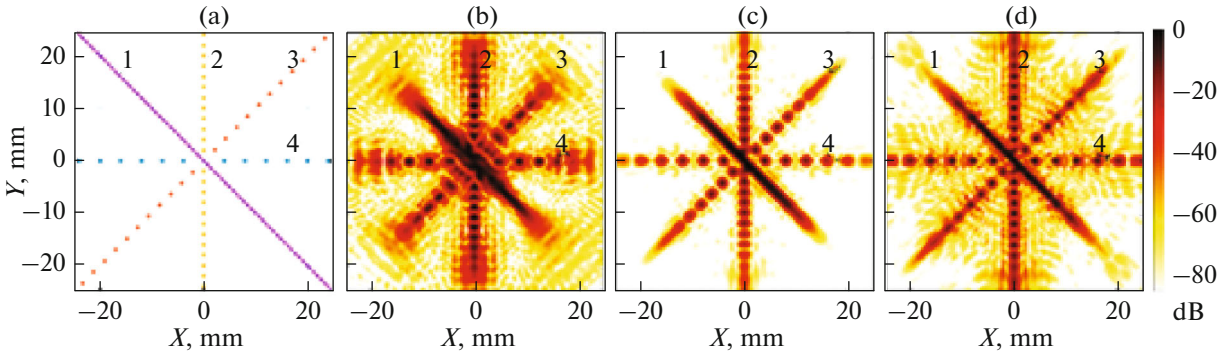

Fig. 1. (a) Specified model location of the point sources. 1, 2, 3, and 4 indicate the axes of location of sources with distances between them of 1, 2, 3, and 4 mm, respectively; reconstructed US images of the point sources using (b) the thin-lens approximation, (c) the Rayleigh integral and (d) the angular spectrum.

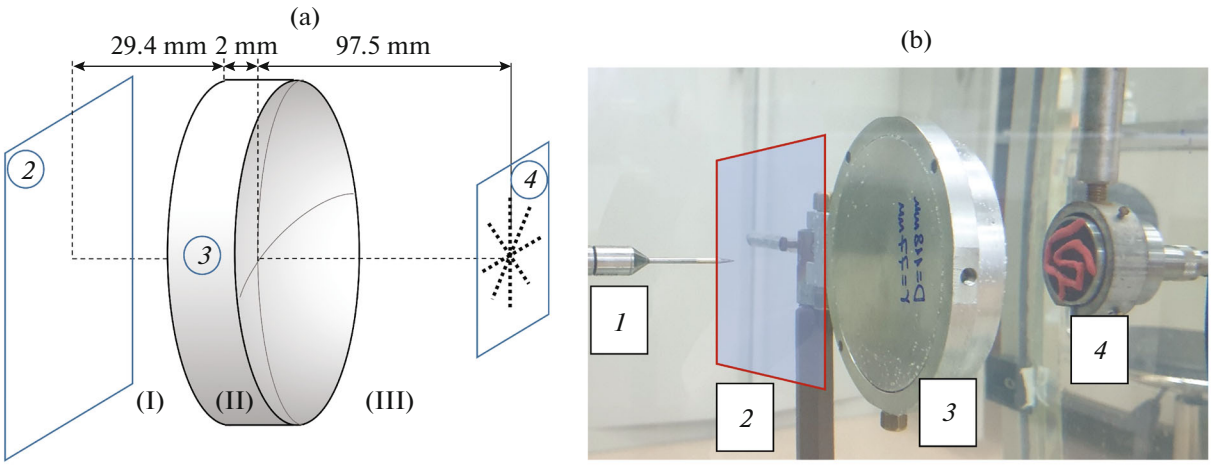

Fig. 2. (a) Geometry of the numerical and physical experiment; (b) picture of the experimental setup. The numbers in (a) and (b) denote (*1*) the needle-shaped hydrophone, (*2*) the surface of the synthetic receiving aperture, (*3*) the plane-concave lens, (*4*) the radiator with the visualized object.

angular spectrum (5), allowing for refraction and the coefficients of transmission through a water/aluminum interface. To consider the coefficient of transmission from medium *1* into medium *2* correctly in solving the inverse problem, the amplitude of the complex pressure of a wave arriving at point (x, y) on the lens surface was not multiplied by coefficient of transmission T_{12} from medium *1* into medium *2*, since it resulted from direct propagation. Instead, it was divided by coefficient of transmission T_{21} from medium *2* into medium *1* in the form

$$T_{21}(x,y) = \frac{2\rho_1 c_1/\cos\varphi_1}{\rho_1 c_1/\cos\varphi_1 + \rho_2 c_2/\cos\varphi_2}, \qquad (9)$$

where φ_1 is the angle of incidence of the reverse wave in the first medium; φ_2 is the angle of refraction in the second medium, calculated using the Snell's law at point (x, y) on the interface between the two media. The coefficient of energy transmission by back propagation was therefore greater than unity because with time inversion, the former reflected wave propagating back was technically added to the wave transmitted through the interface.

At second step (II), we reconstructed the distribution of the complex amplitude of pressure at the concave lens surface, the radius of curvature of which was 77 mm. In the thin-lens approximation, the distribution of the complex amplitude of the pressure obtained at the first step is simply multiplied by corresponding phase factor (8). For aberration-free calculations of the field at the concave lens surface at a distance of 2 mm from its central point, we used Rayleigh integral (2) and an angular spectrum (5). At final step (III), we first calculated the field in the plane located at the distance of 97.5 mm from the lens (where the radiators were located) using Rayleigh integral (3) and angular spectrum (5). The distribution of the real amplitude of the acoustic pressure over this plane is the US image of the point monochromatic sources given in the model.

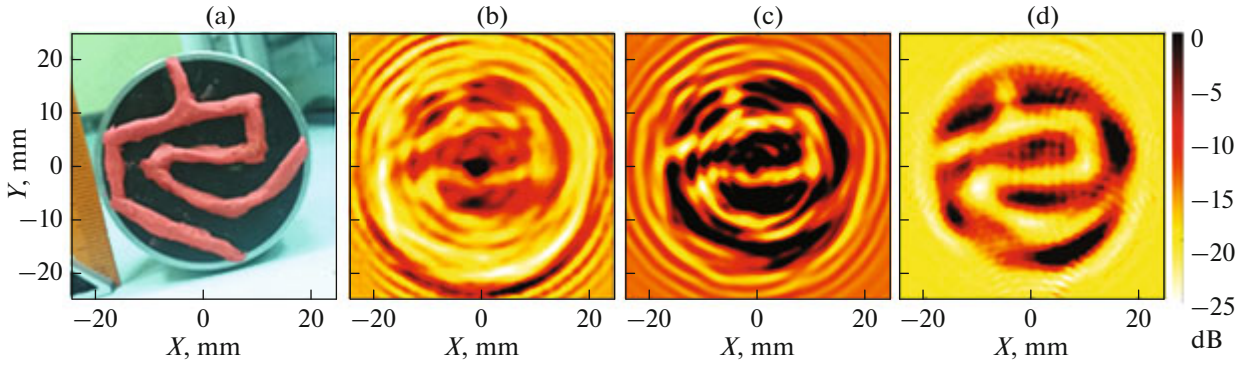

Fig. 3. (a) Image of the radiating surface of the plane radiator with a deposited plasticine object for visualization; US images of the object at the radiator's surface calculated using (b) the thin-lens approximation, (c) the Rayleigh integral, and (d) the angular spectrum.

Figure 1 shows the results from calculating the reconstructed distribution of the amplitude of pressure obtained above. We compared the US images to the original model distribution (Fig. 1a) to determine the quality of reconstruction and estimate the accuracy of our technique. In contrast to the proposed approach, which compensates for aberrations (Figs. 1c, 1d), they clearly distort the image when using the thin-lens approximation (Fig. 1b), especially at some distance from the lens axis.

A comparison of the presented data shows good qualitative and quantitative coincidence between solutions obtained with the proposed approach. This confirms both physical consistency of the solutions and feasibility of using it to solve the problem of reconstructing of the acoustic field distribution in an object's domain and obtain the US image of its profile using the lens system.

RESULTS AND DISCUSSION

For experimental validation of the proposed algorithm, we made measurements in water using an acoustic lens to visualize inhomogeneities at the surface of the acoustic plane radiator. Inhomogeneities were created by depositing sound-absorbing plasticine onto its surface in a specially shaped figure. A V392 broadband radiator (Panametrics, United States) was in the form of a circle plane piezoplate 38 mm in diameter with a matching layer to water with a resonance frequency of 1.5 MHz. It was positioned at the focal length of the lens on the side of the concave surface and coaxially with it (Fig. 2b). The plane-concave lens 118 in diameter was made of aluminum. One surface was a plane and the other was spherical with a radius of curvature of 77 mm. The focal length of this lens was 97.5 mm in the approximation of formula (7). The lens was 2 mm thick at its central point. The acoustic field was detected using a synthetic array antenna on the other side of the lens at a distance of 29.4 mm from its plane surface. The receiving array was synthesized by scanning with a HNA-0400 needle-shaped hydrophone (Onda, United States) controlled by an UMS-3 positioning system (Precision Acoustics, Great Britain) along a surface parallel to the plane lens surface. The lens and radiator remained fixed while scanning. Pulses with 5 periods and frequency 1.5 MHz were excited from a 33250A generator (Agilent, United States) to the radiator. The rate of pulse repetition was 250 Hz. The range of scanning was a square surface with sides of 10 cm, and the scanning step in the lateral direction was 0.5 mm, which was approximately the half-length at the center frequency of the signal. The signals received by the hydrophone were transmitted through a pre-amplifier to a TDS5034B oscilloscope (Tektronix, United States), where they were averaged over 48 samplings for each spatial position of the hydrophone to reduce noises and then saved in the computer's memory for further processing.

Figure 3a shows a picture of the radiator with the deposited pattern. Figure 3b shows the result from reconstructing a US image using the thin-lens approximation. Calculations with the Rayleigh integral and angular spectrum were made for the pulse signal used in the experiment and a set of spectral components in the range from 0.90 to 1.81 MHz with a step of 10 kHz. After an inverse time–frequency Fourier transform, the distribution of the real values of the acoustic pressure was reconstructed directly near the radiator's surface with inhomogeneity in water at different moments. The contour line of the inhomogeneity is clearest at moments with an interval of a half-period of the carrier frequency. Figures 3c, 3d show US images (the real distribution of the acoustic pressure in the logarithmic scale) calculated using the Rayleigh integral and angular spectrum, respectively, at one of these moments when the object was seen with high contrast. The resulting images clearly show the contour line of the inhomogeneity and its sizes, especially when com-

pared to the image obtained in the thin-lens approximation.

CONCLUSIONS

We showed that the use of a solid plane–concave lens allows us to obtain an aberration-free US images of an object immersed in a liquid. A US image was constructed by calculating the acoustic pressure with a Rayleigh integral and an angular spectrum while considering characteristics of the lens and its actual geometry. We demonstrated the effectiveness of these techniques. A comparison showed the good qualitative and quantitative coincidence between the obtained US images and the actual tested object, confirming both physical consistency of the solutions and the feasibility of using the described procedure to solve problems of sonovision in a liquid using a lens system. It should be noted that using Rayleigh integrals and angular spectrum to reconstruct US images through a lens system requires us to consider the shape of the lens. This compensates for aberrations of the lens that affecting the quality of images.

Use of this system allows us to scale the image of a tested object and move it to a required distance. This is useful in applied problems of US imaging in corrosive liquids. It allows us in particular to place the acoustic receiving elements at a considerable distance from a tested object in the domain of the minimized impact of an aggressive environment.

ACKNOWLEDGMENTS

The authors are grateful to V.A. Rozhkov for his help in manufacturing our solid acoustic lens.

FUNDING

This work was supported by the Russian Foundation for Basic Research, project nos. 19-32-90022 and 18-02-00991.

REFERENCES

1. Baikov, S.V., Svet, V.D., and Sizov, V.I., *Acoust. Phys.*, 2000, vol. 46, no. 5, p. 518.
2. Stulenkov, A.V., Korotin, P.I., and Suvorov, A.S., *Bull. Russ. Acad. Sci.: Phys.,* 2020, vol. 84, no. 6, p. 678.
3. Gavrilov, L.R., Sapozhnikov, O.A., and Khokhlova, V.A., *Bull. Russ. Acad. Sci.: Phys.*, 2015, vol. 79, no. 10, p. 1232.
4. Sapozhnikov, O.A., Pishchal'nikov, Yu.A., and Morozov, A.V., *Acoust. Phys.*, 2003, vol. 49, no. 3, p. 354.
5. Stepanishen, P.R. and Benjamin, K.S., *J. Acoust. Soc. Am.*, 1982, vol. 71, p. 803.
6. Kanevskii, I.N., *Fokusirovanie zvukovykh i ul'trazvukovykh voln* (Focusing Sound and Ultrasound Waves), Moscow: Nauka, 1977.
7. Tsysar, S.A., Sinelnikov, E.D., and Sapozhnikov, O.A., *Acoust. Phys.*, 2011, vol. 57, no. 1, p. 94.
8. Sapozhnikov, O.A., Tsysar, S.A., Khokhlova, V.A., and Kreider, W., *J. Acoust. Soc. Am.*, 2015, vol. 138, no. 3, p. 1515.
9. Shenderov, E.L., *Volnovye zadachi gidroakustiki* (Wave Problems of Hydroacoustics), Leningrad: Sudostroenie, 1972.
10. Aldoshina, I.A., *Elektrodinamicheskie gromkogovoriteli* (Electrodynamic Loudspeakers), Moscow: Radio Svyaz', 1989.
11. Vinogradova, M.B., Rudenko, O.V., and Sukhorukov, A.P., *Teoriya voln* (Wave Theory), Moscow: Nauka, 1979.
12. Sapozhnikov, O.A. and Bailey, M.R., *J. Acoust. Soc. Am.*, 2013, vol. 133, no. 2, p. 661.
13. Solimeno, S., Crosignani, B., and di Porto, P., *Guiding, Diffraction, and Confinement of Optical Radiation*, New York: Academic, 1986.

Translated by N. Podymova